Leukemia (2016) **30,** 812–822

www.nature.com/leu

ORIGINAL ARTICLE

Calcineurin and GSK-3 inhibition sensitizes T-cell acute lymphoblastic leukemia cells to apoptosis through X-linked inhibitor of apoptosis protein degradation

V Tosello[1], F Bordin[2], J Yu[3,4,6], V Agnusdei[1], S Indraccolo[1], G Basso[5], A Amadori[1,2] and E Piovan[1,2]

The calcineurin (Cn)–nuclear factor of activated T cells signaling pathway is critically involved in many aspects of normal T-cell physiology; however, its direct implication in leukemogenesis is still ill-defined. Glycogen synthase kinase-3β (GSK-3β) has recently been reported to interact with Cn in neuronal cells and is implicated in *MLL* leukemia. Our biochemical studies clearly demonstrated that Cn was able to interact with GSK-3β in T-cell acute lymphoblastic leukemia (T-ALL) cells, and that this interaction was direct, leading to an increased catalytic activity of GSK-3β, possibly through autophosphorylation of Y216. Sensitivity to GSK-3 inhibitor treatment correlated with altered GSK-3β phosphorylation and was more prominent in T-ALL with Pre/Pro immunophenotype. In addition, dual Cn and GSK-3 inhibitor treatment in T-ALL cells promoted sensitization to apoptosis through proteasomal degradation of X-linked inhibitor of apoptosis protein (XIAP). Consistently, resistance to drug treatments in primary samples was strongly associated with higher XIAP protein levels. Finally, we showed that dual Cn and GSK-3 inhibitor treatment *in vitro* and *in vivo* is effective against available models of T-ALL, indicating an insofar untapped therapeutic opportunity.

Leukemia (2016) **30,** 812–822; doi:10.1038/leu.2015.335

INTRODUCTION

T-cell acute lymphoblastic leukemia (T-ALL) accounts for ~15% of pediatric and 25% of adult cases of ALL. Progress in T-ALL therapy has been impressive, with cure rates approaching 80% for children and 50% for adults;[1,2] however, only limited therapeutic options are available for patients with primary resistant or relapsed disease.

Calcineurin (PPP3; PP2B referred to as Cn) is a calcium-activated serine/threonine phosphatase, composed of a catalytic subunit (PPP3CA) and a regulatory subunit (PPP3CB), critical to a number of developmental processes in the cardiovascular, nervous and immune system. Cn has the ability to dephosphorylate a broad range of proteins, including nuclear factor of activated T cell (NFAT) proteins. Although critically involved in many aspects of normal T-cell survival, proliferation and activation, the direct implication of Cn and/or its downstream NFAT targets in lymphomagenesis and cancer in general has only recently been reported.[3,4] Available evidence shows that NFAT transcription factors are mediators of Cn action in different cancers.[5–7] However, it is possible that NFAT factors are not the only targets of Cn in leukemogenesis, as Cn can dephosphorylate other factors possibly relevant to its oncogenic properties. Glycogen synthase kinase-3β (GSK-3β) has recently been reported to interact with PPP3CA in neuron-derived cells[8] and is implicated in *MLL* rearranged leukemia.[9] Interestingly, we found Cn to be able to directly interact with and participate in activation of GSK-3β. GSK-3 is a serine/threonine protein kinase ubiquitously expressed and at variance with the majority of kinases is constitutively active, and is functionally inactivated after phosphorylation by various kinases in response to different stimuli.[10] As little is currently known about the significance of GSK-3β to T-ALL cell survival and pathobiology, and the functional interaction between GSK-3β and Cn has not been reported previously in T-ALL, we pursued the functional impact of this axis in the present study.

MATERIALS AND METHODS

Inhibitors and drugs

BIO (6-bromoindirubin-3′-oxime), Tideglusib (NP-12), SB216713 and Embelin were from Selleck Chemicals LLC (Houston, TX, USA). CN585 (6-(3,4-dichlorophenyl)-4-(*N*,*N*-dimethylaminoethylthio)-2-phenyl-pyrimidine) was from Merck Millipore (Merck, Damstadt, Germany). Cyclosporin A (CsA), ionomycin, FK506 and MG132 (Z-Leu-Leu-Leu-al) were from Sigma-Aldrich (Saint Louis, MO, USA).

Cell lines and primary leukemia samples, constructs and molecular cloning, *in vitro* kinase assays and phosphorylation analysis, *in vitro* histidin-pull-down protein interaction assays, transfection and immunoprecipitation (IP) in 293 T cells, western blotting and IP, preparation of cytoplasmic and nuclear extracts, enzyme-linked immunosorbent assay for NFAT2 DNA-binding activity, ubiquitination detection, cell viability assays and flow cytometry, human apoptosis array, lentiviral constructs and viral production, GSK-3β *in vitro* kinase assay, quantitative real-time PCR, xenografts and treatment studies, molecular characterization of T-ALL samples and statistical analyses are detailed in Supplementary Materials and Methods.

[1]UOC Immunologia e Diagnostica Molecolare Oncologica, Istituto Oncologico Veneto IOV-IRCCS, Padova, Italy; [2]Dipartimento di Scienze Chirurgiche, Oncologiche e Gastroenterologiche, Universita' di Padova, Padova, Italy; [3]Department of Biomedical Informatics, Columbia University, New York, NY, USA; [4]Department of Systems Biology, Columbia University, New York, NY, USA and [5]Dipartimento di Salute della Donna e del Bambino, Università di Padova, Padova, Italy. Correspondence: Dr E Piovan, Dipartimento di Scienze Chirurgiche, Oncologiche e Gastroenterologiche, Universita' di Padova, via Gattamelata, 64, Padova 35128, Italy.
E-mail: erich.piovan@unipd.it
[6]Current address: Department of Precision Medicine, Oncology Research Unit, Pfizer Inc., Pearl River, NY 10965, USA.
Received 1 September 2015; revised 20 November 2015; accepted 24 November 2015; accepted article preview online 9 December 2015; advance online publication, 8 January 2016

RESULTS

Cn directly interacts with GSK-3β and modulates its activity

GSK-3β has recently been reported to interact with PPP3CA in neuron-derived cells.[8] We thus investigated whether this interaction was also present in T-ALL cells. To this end, we lysed Jurkat T-ALL cells and executed IP against PPP3CA and subsequently immunoblotting anti-GSK-3β. Effectively, the two endogenous proteins (GSK-3β and PPP3CA) were found to interact in T-ALL cells (Figure 1a). To study further the functional interaction between these two proteins, we transfected HEK 293T cells with full-length FLAG-tagged PPP3CA and full-length hemagglutinin-tagged GSK-3β. Forty hours post transfection, cells were treated with ionomycin (to activate Cn/NFAT signaling), CsA (to inactivate Cn/NFAT signaling) or vehicle control for 1 h. Cells were then lysed and subjected to IP with anti-FLAG beads. The interaction between PPP3CA and GSK-3β present under basal conditions was increased following acute activation of Cn by ionomycin (Figure 1b). On the other hand, CsA treatment did not modify this basal interaction. Histidine-pulldown experiments using histidin-tagged PPP3CA and glutathione *S*-transferase (GST)-tagged GSK-3β demonstrated that GSK-3β and PPP3CA could directly interact *in vitro* (Figure 1c).

To address the possible functional interaction between these two proteins with opposing biochemical functions, we executed *in vitro* phosphorylation and dephosphorylation assays. Unexpectedly, *in vitro* kinase assays showed that PPP3CA could significantly increase GSK-3β phosphorylation (Figure 1d), whereas we did not detect any significant phosphorylation of PPP3CA by GSK-3β (data not shown). Altered phosphorylation of GSK-3β in the presence of PPP3CA, including increased phosphorylation of tyrosine 216 (Y216), was confirmed by mass spectrometry (Supplementary Table S1). Increased GSK-3β phosphorylation at Y216 was further confirmed by immunoblotting (Figure 1e). Phosphorylation of GSK-3β at Y216 increases its enzymatic activity and could be involved in autophosphorylation.[11] Interestingly, the increased level of phosphorylation of GSK-3β in the presence of PPP3CA was

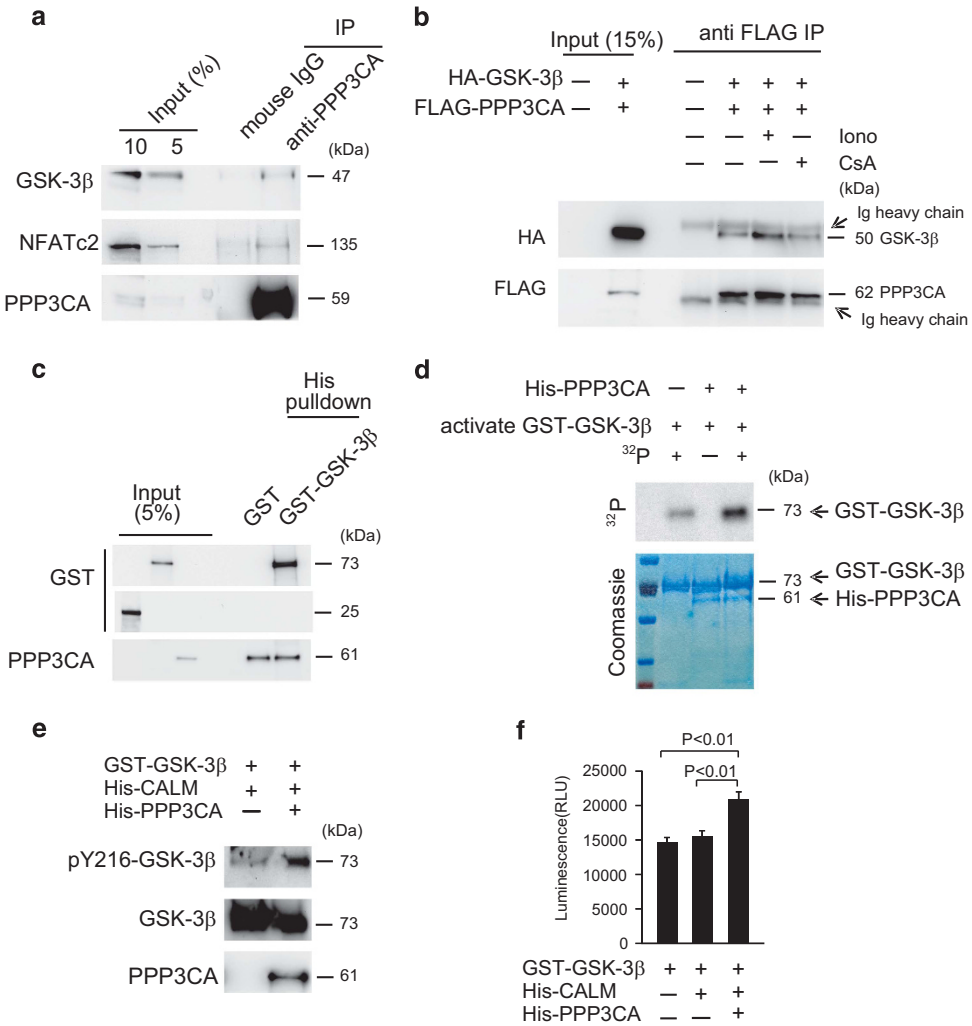

Figure 1. PPP3CA interacts with GSK-3β and regulates GSK-3β catalytic activity and phosphorylation. (**a**) Immunoblot analysis of GSK-3β and NFATc2 after PPP3CA protein immunoprecipitation in Jurkat T-ALL cells. (**b**) Analysis of GSK-3β–PPP3CA interaction via immunoblot analysis of protein complexes recovered after FLAG immunoprecipitation under basal conditions and after treatment with ionomycin (Iono) or cyclosporine (CsA). (**c**) Analysis of GSK-3β–PPP3CA interaction via immunoblot analysis of protein complexes recovered after histidin-tagged PPP3CA (His-PPP3CA) pulldown of recombinant glutathione *S*-transferase (GST)-tagged GSK-3β (GST-GSK-3β). (**d**) *In vitro* kinase analysis of GSK-3β phosphorylation in the absence and in the presence of recombinant PPP3CA (His-PPP3CA) protein. Top panel shows ^{32}P autoradiography after SDS-polyacrylamide gel electrophoresis and corresponding protein loading is shown at the bottom. (**e**) Immunoblot analysis of phospho Y216 (pY216) GSK-3β in recombinant protein mixtures containing recombinant GST-GSK-3β with or without recombinant His-PPP3CA and His-Calmodulin (CALM). (**f**) GSK-3β kinase activity in *in-vitro* protein mixtures containing recombinant GST-GSK-3β with or without recombinant His-PPP3CA and His-Calmodulin (CALM). Error bars represent ± s.d. for triplicate experiments.

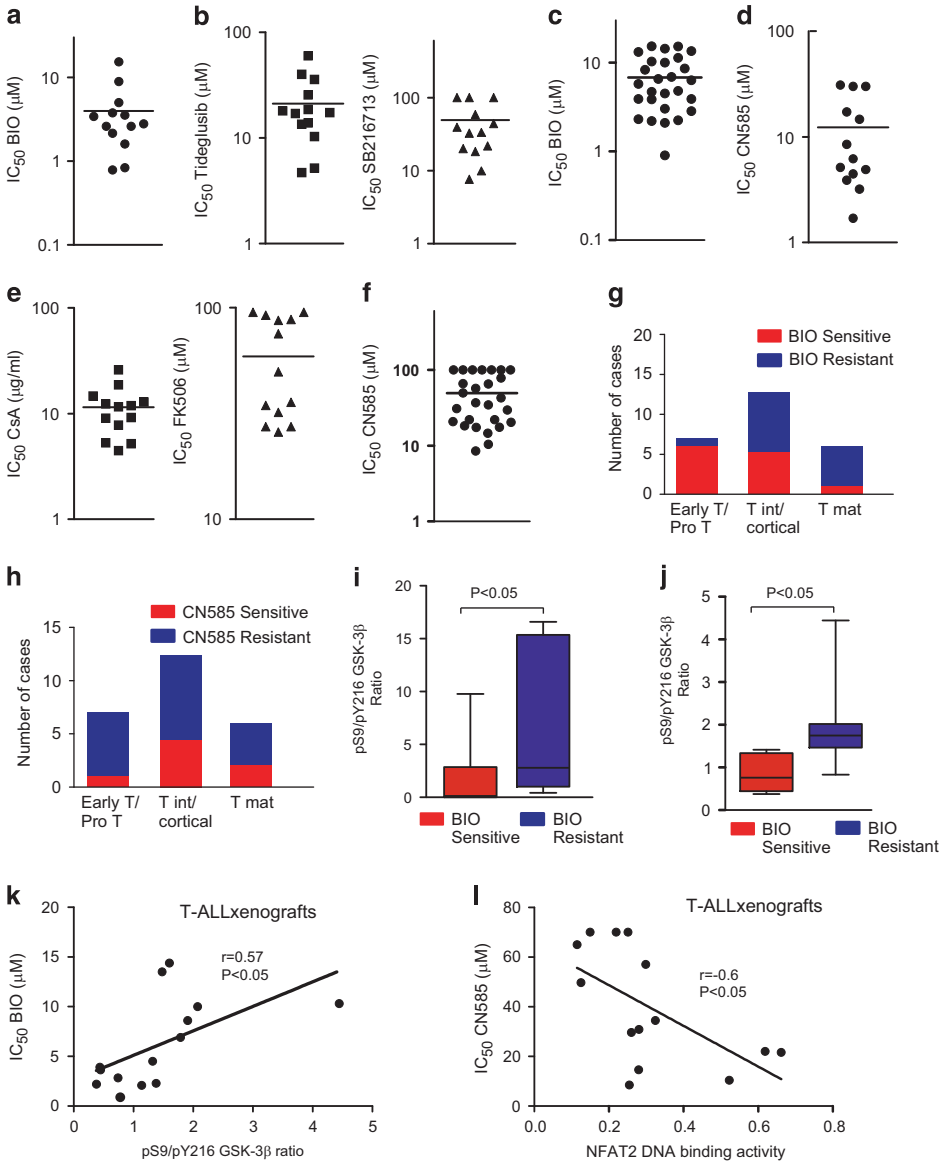

Figure 2. Sensitivity to pharmacological inhibition of Cn and GSK-3 in T-ALL cells. (**a**) IC_{50} values for the GSK-3 inhibitor BIO in T-ALL cell lines ($n=13$). Bar represents mean value. (**b**) IC_{50} values for additional GSK-3 inhibitors (Tideglusib and SB216713) in T-ALL cell lines. Bar represents mean value. (**c** and **f**) Patient samples are classified based on their immunophenotype in pro-, pre-, cortical and mature T-ALL. (**c**) IC_{50} values for GSK-3 inhibitor BIO in T-ALL xenografts ($n=27$). Bar represents mean value. (**d**) IC_{50} values for the Cn inhibitor CN585 in T-ALL cell lines. Bar represents mean values. (**e**) IC_{50} values for additional Cn inhibitors (CsA and FK506) in T-ALL cell lines. Bars represent mean values. (**f**) IC_{50} values for Cn inhibitor CN585 in T-ALL xenografts ($n=27$). Bar represents mean value. (**g**) Comparison of response to BIO (sensitive: $IC_{50} < 5$ μM, resistant: $IC_{50} > 5$ μM) and (**h**) response to CN585 (sensitive: $IC_{50} < 20$ μM, resistant: $IC_{50} \geqslant 20$ μM) in immunophenotype distinct T-ALL subgroups. (**i**) Box plot of pS9/pY216 GSK-3β ratio in BIO-sensitive ($IC_{50} < 3.5$ μM) and BIO-resistant ($IC_{50} > 3.5$ μM) T-ALL cell lines. The box plot whiskers extend from the lowest to the highest values. (**j**) Box plot of pS9/pY216 GSK-3β ratio in BIO-sensitive ($IC_{50} < 5$ μM) and BIO-resistant ($IC_{50} > 5$ μM) T-ALL xenografts. The box plot whiskers extend from the lowest to the highest values. (**k**) Correlation between IC_{50} values for BIO and pS9/pY216 GSK-3β ratios in T-ALL xenografts ($n=14$). (**l**) Correlation between IC_{50} values for CN585 and NFAT2 DNA-binding activity in T-ALL xenograft nuclear extracts ($n=14$).

paralleled by a modest increase in GSK-3β enzymatic activity *in vitro* (Figure 1f).

Immature immunophenotype and low pS9/pY216 GSK-3β ratio correlates with sensitivity to GSK-3 inhibitor treatment in T-ALL cells

Our results point to a functionally important interaction between Cn/NFAT and GSK-3 signaling pathways that could be potentially exploited therapeutically in T-ALL. To address this question we tested the effects of the GSK-3-specific inhibitor BIO on the viability of numerous T-ALL cell lines ($n=13$). Inhibitor dose escalation resulted in higher cytotoxicity in most cell lines tested. Their viability was inhibited by BIO at a half-maximal inhibitory dose (IC_{50}) < 5 μM for most T-ALL cell lines (10/13; Figure 2a and Supplementary Figure S1), a concentration comparable to that which promotes expansion of hematopoietic stem cells *in vitro*.[12] Further studies with additional GSK-3 inhibitors such as Tideglusib/NP-12 (recently described non-ATP-competitive inhibitor with relatively higher IC_{50} than BIO) and SB216713, confirmed that a considerable fraction of T-ALL cell lines were sensitive to GSK-3 inhibition (Figure 2b). Similarly, evaluation of the effects of

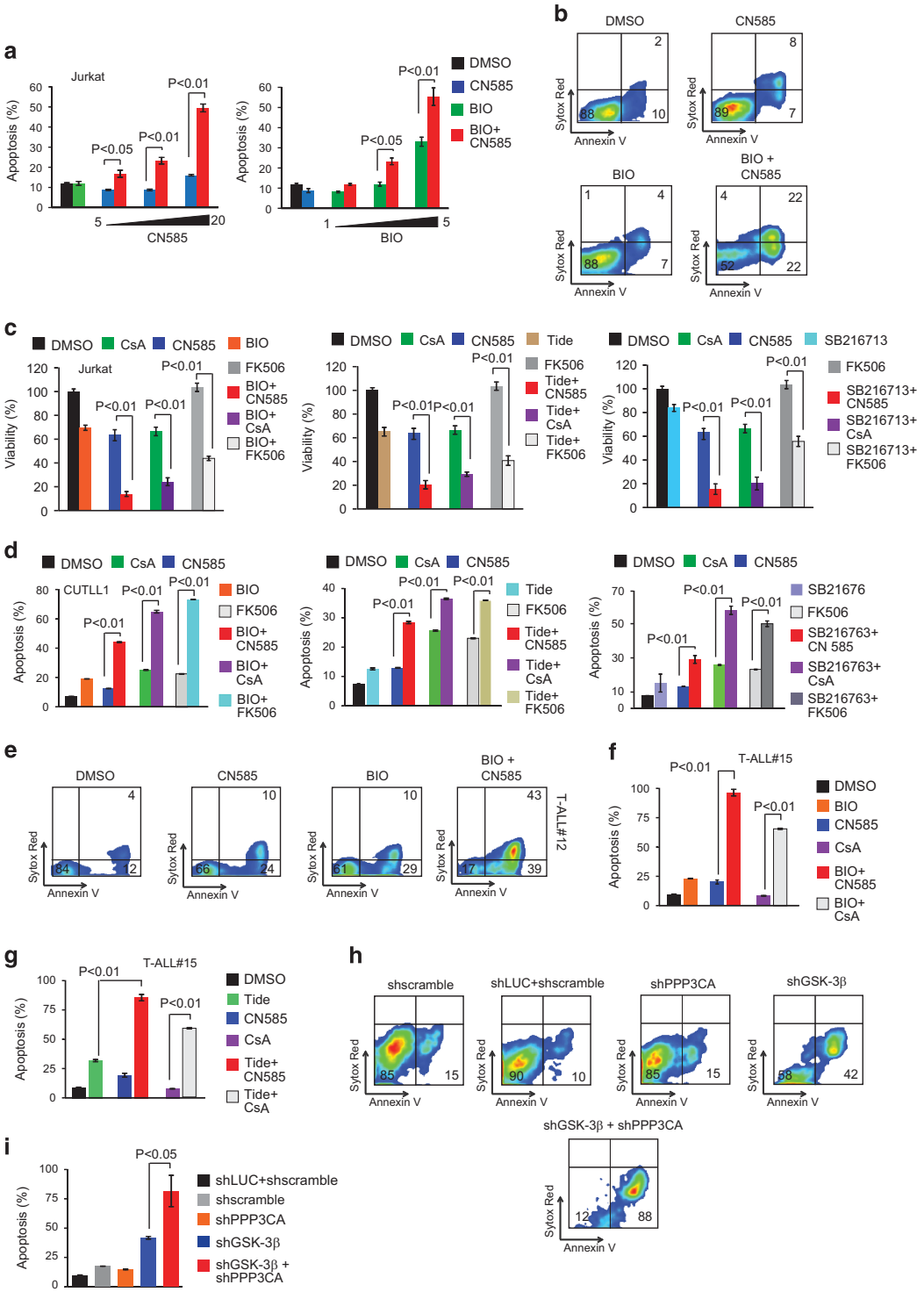

Figure 3. Joint pharmacologic inhibition of Cn and GSK-3 induces a synergistic anti-leukemic effect. (**a**) Apoptotic quantification in Jurkat T-ALL cells treated *in vitro* with vehicle only, CN585 alone (5–20 μM; left panel), BIO (1–5 μM; right panel) alone or BIO (1–5 μM) plus CN585 (5–20 μM). Error bars represent ± s.d. for triplicate experiments. (**b**) Representative plots of apoptosis in Jurkat T-ALL cells treated *in vitro* with vehicle only, BIO (2 μM), CN585 (20 μM) or BIO plus CN585 (BIO+CN585; 2 and 20 μM, respectively). (**c**) Cell viability quantification in Jurkat cells treated for 72 h *in vitro* with vehicle only, CN585 (10 μM), CsA (10 μg/ml), FK506 (20 μM), BIO (3 μM), Tideglusib (15 μM) and SB216713 (20 μM) in various combinations. Error bars represent ± s.d. of triplicate experiments. (**d**) Quantification of apoptosis in CUTLL1 cells treated *in vitro* with vehicle only, CN585 (5 μM), CsA (7.5 μg/ml), FK506 (15 μM), BIO (1 μM), Tideglusib (15 μM) and SB216713 (7.5 μM) in various combinations. Error bars represent ± s.d. of triplicate experiments. (**e**) Representative plots of apoptosis in T-ALL#12 xenograft cells treated *in vitro* with vehicle only, CN585 (20 μM), BIO (3 μM) or BIO plus CN585 (BIO+CN585; 3 and 20 μM, respectively). (**f** and **g**) Quantification of apoptosis in T-ALL#15 xenograft cells treated *in vitro* with vehicle only, BIO (5 μM), CN585 (15 μM), CsA (10 μg/ml) and Tideglusib (10 μM) in various combinations. Error bars represent ± s.d. of triplicate experiments. Representative plots of apoptosis (**h**) and apoptosis quantification (**i**) in Jurkat cells transduced with control vectors (shscramble or shLUC), vector containing short hairpin RNA (shRNA) sequences against PPP3CA (shPPP3CA), vector containing shRNA sequences against GSK-3β (shGSK-3β) or both shPPP3CA and shGSK-3β.

GSK-3 inhibition by BIO on T-ALL xenograft viability disclosed that around 40% of primary xenografts (12/27) had an IC_{50} <5 μM (Figure 2c and Supplementary Figure S1). Next, we evaluated the sensitivity of these same T-ALL cell lines to the selective Cn inhibitor, CN585. Again, some cell lines ($n=8$; IC_{50} <10 μM) were sensitive to Cn inhibition (Figure 2d and Supplementary Figure S1), whereas other cell lines ($n=5$; IC_{50} >15 μM) were resistant. Further studies using additional Cn inhibitors such as CsA and FK506 confirmed that a sizable fraction of T-ALL cell lines were responsive to Cn inhibition (see Figure 2e). Similarly, a

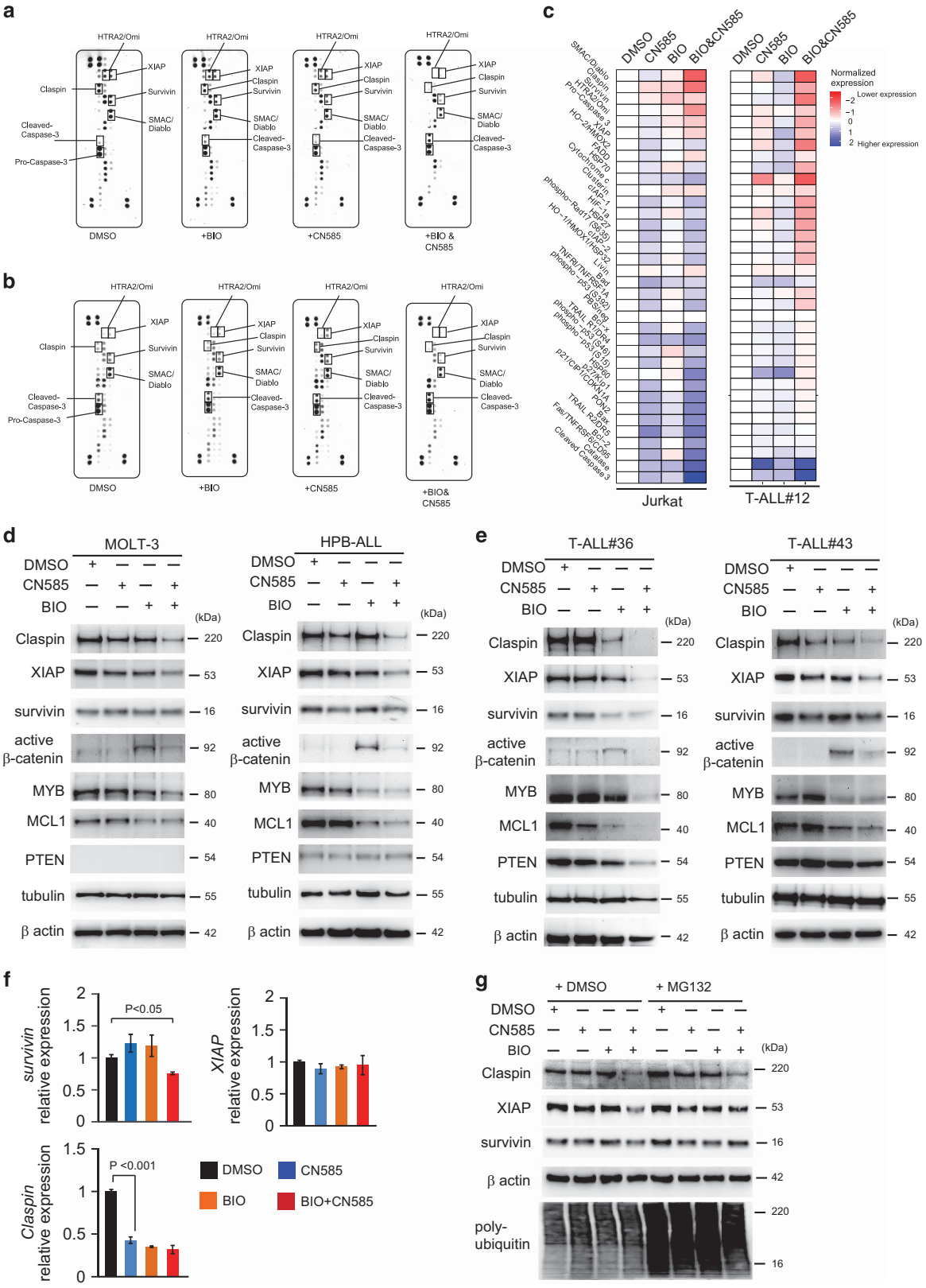

subgroup of T-ALL xenografts were found to be responsive to Cn inhibition by CN585 (Figure 2f and Supplementary Figure S1; $n=7$; IC_{50} $<20\,\mu M$). All together, these results imply that a subset of T-ALL cell lines and xenografts are relatively sensitive to GSK-3 and Cn inhibition.

Immunophenotypical classification of T-ALLs based on expression of surface markers differentially expressed during T-cell development can be used to distinguish three main subgroups of T-ALL: (i) pro/pre-T ALL, (ii) thymic/cortical T-ALL and (iii) mature T-ALL.[13] T-ALL cell line and xenograft molecular characteristics are shown in Supplementary Figure S2. We assessed whether sensitivity or resistance to each single drug treatment correlated with a particular subgroup of T-ALL. Interestingly, the pro/pre T-ALL subgroup was associated with greater sensitivity (IC_{50} $<5\,\mu M$) to GSK-3 inhibition (Figures 2g and h, and Supplementary Figure S1) but at the same time was associated with resistance to Cn inhibition. On the whole, these results identify the more immature pro/pre T-ALL subgroup as the most amenable T-ALL subgroup for targeting of GSK-3.

T-ALL cell lines (Figure 2i and Supplementary Figure S3) and primary samples (Figure 2j and Supplementary Figure S3), which were responsive to GSK-3 inhibition (IC_{50} <3.5 and $<5\,\mu M$, respectively), were found to have significantly lower ratios of pS9/pY216 GSK-3β compared with low responders (IC_{50} >3.5 or $>5\,\mu M$, respectively; $P<0.05$ for T-ALL cell lines and primary samples). Moreover, we observed a positive correlation between BIO IC_{50} values and pS9/pY216 GSK-3β ratio in T-ALL cell lines (Spearman's $r=0.74$, P <0.05; Supplementary Figure S3) and primary TALL xenografts (Spearman's $r=$ 0.57, P <0.05; Figure 2k). On the other hand, we observed a negative correlation between CN585 IC_{50} values and NFAT2 DNA-binding activity in T-ALL cell lines (Spearman's $r=-0.69$, P <0.05; Supplementary Figure S3) and primary T-ALL xenografts (Spearman's $r=-0.6$, P <0.05; Figure 2l).

Joint *in vitro* inhibition of GSK-3 and Cn induces strong anti-leukemic effects in T-ALL cells

To address whether the modulation of GSK-3β activity by Cn could be exploited therapeutically, we evaluated whether joint *in vitro* inhibition of the two pathways could have an additive/synergistic effect, especially in partially resistant samples. To this end, T-ALL cell lines and primary T-ALL xenografts were treated with vehicle, GSK-3 inhibitor (BIO), Cn inhibitor (CN585) or the combination BIO and CN585, and evaluated for apoptosis (48 h) or loss of viability (72 h). Jurkat cells treated with increasing doses of CN585 or BIO showed an enhanced apoptotic response and loss of viability with the combination treatment compared with each single drug only (Figures 3a and b). Analysis of drug interactions using the median-effect method of Chou and Talay[14] to calculate the combination index, disclosed a synergistic anti-leukemic effect in the combination BIO and CN585 (combination index <1) at multiple concentrations (Supplementary Figure S4). Synergistic effects were obtained using additional GSK-3 inhibitors (Tideglusib and SB216763) and Cn inhibitors (CsA and FK506; Figure 3c and Supplementary Figure S4). Similarly, CUTLL1 (Figure 3d) and MOLT4 (Supplementary Figure S4) T-ALL cells showed a similar effect with enhanced apoptotic response and/or loss of viability with the combination treatment compared with each single drug only. Similar results with the combination BIO and CN585 were obtained in 10 different T-ALL xenografts (Figures 3e–g and Supplementary Figure S4, and data not shown). Notably, the anti-leukemic effects of the combination treatment (BIO and CN585) were prominent also in primary tumor samples, which were highly resistant to the single treatments (Supplementary Figure S4 and data not shown). Similar results were obtained with the GSK-3 inhibitor Tideglusib and Cn inhibitor CsA (Figures 3f and g, and Supplementary Figure S4).

Further, to demonstrate that the observed synergistic apoptotic effect seen using GSK-3 and Cn inhibitors is effectively due to the inhibition of GSK-3β and Cn, we knocked down GSK-3β and PPP3CA in Jurkat T-ALL cells. We found that severe knockdown of GSK-3β determined an increase in spontaneous apoptosis, which was further increased by concomitant knockdown of PPP3CA (Figures 3h and I, and Supplementary Figure S4).

The anti-leukemic effect of joint inhibition of GSK-3 and Cn is mediated through the downregulation of multiple anti-apoptotic proteins including X-linked inhibitor of apoptosis protein (XIAP)

To assess which survival factors were responsible for the strong anti-leukemic effects of the combination treatment BIO and CN585, we used antibody-based apoptosis arrays. To this end, Jurkat cells and a primary T-ALL xenograft (T-ALL#12) were treated for 24 h with vehicle, BIO, CN585 or the combination CN585 plus BIO. Cell lysates were then hybridized to human apoptosis arrays, which allow the simultaneous detection of 35 apoptosis-related proteins. In Jurkat cells, the combination treatment BIO and CN585 determined a strong induction of cleaved Caspase 3, which was associated with a marked reduction in numerous anti-apoptotic proteins including XIAP, survivin, claspin and clusterin (Figures 4a and c). Similar results were obtained in a primary T-ALL xenograft (Figures 4b and c), where XIAP, survivin and claspin were all downregulated in the combination treatment. Human apoptosis array results for some of the most differentially regulated anti-apoptotic proteins were validated by immunoblotting in these samples (Supplementary Figure S5). Further analysis in four other T-ALL cell lines (Figure 4d and Supplementary Figure S5) and three other primary samples (Figure 4e and Supplementary Figure S5) disclosed that XIAP and claspin were consistently downregulated in all cases, whereas survivin downregulation was less consistent. Other GSK-3 targets proposed to have a role in mediating GSK-3 function in other cellular systems such as PTEN (phosphatase and tensin homolog), MCL1, β-catenin and c-Myb[15] were also found to be partially modulated; however, joint inhibition of Cn with CN585 did not consistently further modulate their levels (Figures 4d and e, and Supplementary Figure S5). XIAP

Figure 4. Anti-leukemic effect of joint pharmacologic inhibition of Cn and GSK-3 is mediated through the downregulation of multiple anti-apoptotic proteins including claspin, XIAP and survivin. Whole-cell extracts from Jurkat T-ALL (**a**) or T-ALL#12 (**b**) cells treated for 24 h with vehicle only, BIO (5 or 2.5 μM), CN585 (20 μM) or BIO plus CN585 (BIO+CN585; 5 or 2.5 and 20 μM, respectively) in combination were hybridized to human apoptosis arrays. Apoptotic proteins that were consistently modulated are labeled. (**c**) Heat map representation of apoptotic protein expression from **a** and **b**. (**d**) Western blot analysis of claspin, XIAP, survivin, active β-catenin, c-MYB, MCL1 and PTEN expression in MOLT-3 and HPB-ALL cell lines treated for 24 h with vehicle only, BIO (3–5 μM), CN585 (20 μM) or BIO plus CN585 (BIO+CN585; 3–5 and 20 μM, respectively). Tubulin and β-actin are shown as loading controls. (**e**) Immunoblot analysis of claspin, XIAP, survivin, active β-catenin, c-MYB, MCL1 and PTEN expression in T-ALL 36 and 43 treated for 24 h with vehicle only, BIO (2.5–10 μM), CN585 (20 μM) or BIO plus CN585 (BIO+CN585; 2.5–10 and 20 μM, respectively). Tubulin and β-actin are shown as loading controls. (**f**) Quantitative reverse-transcriptase PCR evaluation of *Claspin*, *XIAP* and *Survivin* expression in Jurkat cells treated for 8 h with vehicle only, BIO (5 μM), CN585 (20 μM) or BIO plus CN585 (BIO+CN585; 5 and 20 μM, respectively). Error bars represent ± s.d. for triplicate experiments. (**g**) Immunoblot analysis of claspin, XIAP and survivin expression in Jurkat cells treated for 8 h with the indicated drugs in the presence or in the absence of the proteasomal inhibitor MG132. β-Actin is shown as a loading control, while polyubiquitin ladder indicates inhibition of proteasomal degradation by MG132.

is often overexpressed in malignant cells and elevated levels of XIAP increase resistance to apoptosis induced by both mitochondrial and death receptor cascades.[16] Similarly, we find that XIAP is consistently downregulated in tumor samples responding to joint GSK-3 and Cn inhibition, suggesting a critical role for this protein in regulating sensitivity to these drug treatments. We initially evaluated whether XIAP down-regulation following joint GSK-3 and Cn inhibition was mediated through a transcriptional or posttranscriptional mechanism. *XIAP* mRNA levels did not change following joint GSK-3 and Cn inhibition, whereas both *Survivin* and *Claspin* mRNA levels were significantly reduced (Figure 4f), suggesting that decreased XIAP is not due to inhibition of *XIAP* transcription. To examine whether reduced XIAP expression was dependent on proteasome-mediated protein degradation,[17] Jurkat cells were treated with CN585, BIO or the combination in the presence or absence of the proteasome inhibitor MG132. Indeed, MG132 was able to substantially rescue XIAP and survivin downregulation (Figure 4g), while it had no effect on claspin expression, probably because transcriptional downregulation and caspase-mediated degradation of claspin represent the predominant mechanisms of its reduced expression. In addition, we found that GSK-3 inhibition (and especially in combination with Cn inhibition) promoted the ubiquitination of XIAP, illustrated by that IP of XIAP from BIO- or BIO+CN585-treated cells identified the association of ubiquitin with XIAP (Supplementary Figure S5). All together, these results suggest that joint GSK-3 and Cn inhibition decrease XIAP expression through increased proteasome-mediated protein degradation.

XIAP protein levels are critical for regulating the apoptotic response to inhibition of GSK-3 and Cn

We next evaluated the effects of targeted modulation of XIAP expression on the sensitivity of T-ALL cells to GSK-3 and Cn inhibitors. Lentiviral-mediated overexpression of XIAP in two BIO- and CN585-sensitive cell lines RPMI 8402 (Figure 5a) and CCRF-HSB2 (Supplementary Figure S6) revealed that XIAP-overexpressing cells were rendered remarkably resistant to the combination treatment BIO and CN585. Consistently, lentiviral-mediated knockdown of XIAP using two independent hairpins in two BIO- and CN585-resistant cell lines Jurkat (Figure 5c) and CCRF-CEM (Supplementary Figure S6) rendered these cells exquisitely sensitive to the combination treatment BIO and CN585. In addition, pharmacological suppression of XIAP expression by Embelin also determined a dramatic increase in response to the combination treatment BIO and CN585 (Figure 5d). All together, these results imply that XIAP protein levels are critical in regulating the cellular response to the drug treatments BIO and CN585. Coherently, analysis of XIAP protein expression across primary T-ALL xenografts revealed that XIAP levels were significantly higher in T-ALL samples, which were resistant to both inhibitors compared with samples sensitive to at least one of the drug treatments (Figures 5e and f).

Joint *in- vivo* inhibition of GSK-3 and Cn exhibit a strong anti-leukemic effect

CN585 is a recently developed Cn-specific inhibitor, with improved toxicity profile than classical Cn inhibitors such CsA and FK506, owing to its inability to inhibit immunophillins.[18] Preliminary experiments disclosed that a dose of 30 mg/kg of CN585 was effective at inhibiting Cn/NFAT signaling *in vivo* (data not shown). To test the efficacy of combined GSK-3 and Cn inhibition *in vivo*, we generated *NOTCH1*-driven T-ALL tumors by infecting hematopoietic progenitors with retroviruses expressing a mutant constitutively active form of the NOTCH1 receptor (*NOTCH1* L1601P ΔPEST).[19] We found these tumors to be sensitive to GSK-3 inhibition by BIO (IC_{50} $< 2\,\mu M$) and Cn inhibition by CN585 (IC_{50} $< 10\,\mu M$). Similar to what was observed in human T-ALL cell lines and primary xenografts, the combination treatment (BIO and CN585) was highly synergistic *in vitro* (Figure 6a and Supplementary Figure S7), with combination index < 1 at multiple concentrations. Similar results were obtained using the GSK-3 inhibitor Tideglusib and the Cn inhibitor CsA (Figure 6b and Supplementary Figure S7). Next, we infected *NOTCH1*-induced T-ALL lymphoblasts with a luciferase-expressing retrovirus and transplanted them into secondary recipients. To test the efficacy of BIO and CN585 in combination, we treated mice transplanted with *NOTCH1*-murine tumors expressing luciferase with vehicle only (dimethylsulfoxide), BIO, CN585 or BIO plus CN585 and monitored their response to therapy by *in-vivo* bioimaging. Owing to sensitization of mice to the side effects of joint GSK-3 and Cn inhibition, including diarrhea and sudden death, we had to alternate single drug treatments. Animals treated with BIO or CN585 in this experiment showed modest anti-tumor responses or progressive tumor growth similar to that observed in vehicle-treated controls, whereas mice treated with BIO plus CN585 showed significant anti-tumor responses (Figures 6c and d, and Supplementary Figure S7; $P < 0.05$), which translated into significantly improved survival in this group (Supplementary Figure S7; $P < 0.05$).

To further test the efficacy of this treatment combination *in vivo*, we established leukemia xenografts in nonobese diabetic/severe combined immunodeficiency IL2Rγ^{null} mice using a primary T-ALL sample infected with lentiviruses expressing the luciferase gene. Animals were treated with vehicle only (dimethylsulfoxide), BIO, CN585 or BIO plus CN585 starting 3 days after transplantation (prior confirming homogeneous tumor engraftment by bioimaging). Mice treated with BIO or CN585 showed modest tumor growth retardation compared with vehicle-treated controls, which showed progressive tumor growth, whereas mice treated with CN585 plus BIO showed significant anti-tumor responses (Figures 6e and f), which translated into significantly improved survival in this group (Supplementary Figure S7; $P < 0.05$).

To further test the efficacy of this treatment combination *in vivo* and its possible future feasibility in human clinical trials, we made use of the clinically relevant GSK-3 inhibitor Tideglusib (NP-12) and Cn inhibitor CsA. We established leukemia xenografts in nonobese diabetic/severe combined immunodeficiency IL2Rγ^{null} immunodeficient mice using a primary T-ALL sample infected with lentiviruses expressing the luciferase gene. Animals harboring homogeneous tumor burdens by *in vivo* bioimaging were treated with vehicle only (dimethylsulfoxide), NP-12, CsA or NP-12 plus CsA. In this experiment, mice treated with NP-12 or CsA showed some degree of tumor growth inhibition compared with that observed in vehicle-treated controls, whereas mice treated with NP-12 plus CsA showed significant anti-tumor responses (Supplementary Figure S7).

DISCUSSION

GSK-3 has recently been implicated in *MLL* rearranged leukemia[9] and has been reported to interact with PPP3CA in neuronal cells.[8] In addition, GSK-3 was found among the most prevalent PPP3CA-interacting proteins isolated by mass spectrometry from Jurkat T-ALL cells (data not shown), is potentially druggable and its significance in T-ALL cell survival remains to be determined. These findings make GSK-3 an interesting candidate to pursue further. GSK-3β is known to antagonize Cn in various cells including T cells[20] and neurons[21] by negatively regulating NFAT-dependent gene expression. GSK-3 activity is generally high in resting cells and is regulated in several ways: by inhibitory phosphorylation at GSK-3β/α S9/21; by activating phosphorylation on GSK-3β/α Y216/Y279; by subcellular localization; and by binding to scaffold proteins in multimeric complexes.[22] The phosphorylation state of these residues is dynamic and highly modulated. In fact, although protein phosphatase-1 is implicated in GSK-3 dephosphorylation,

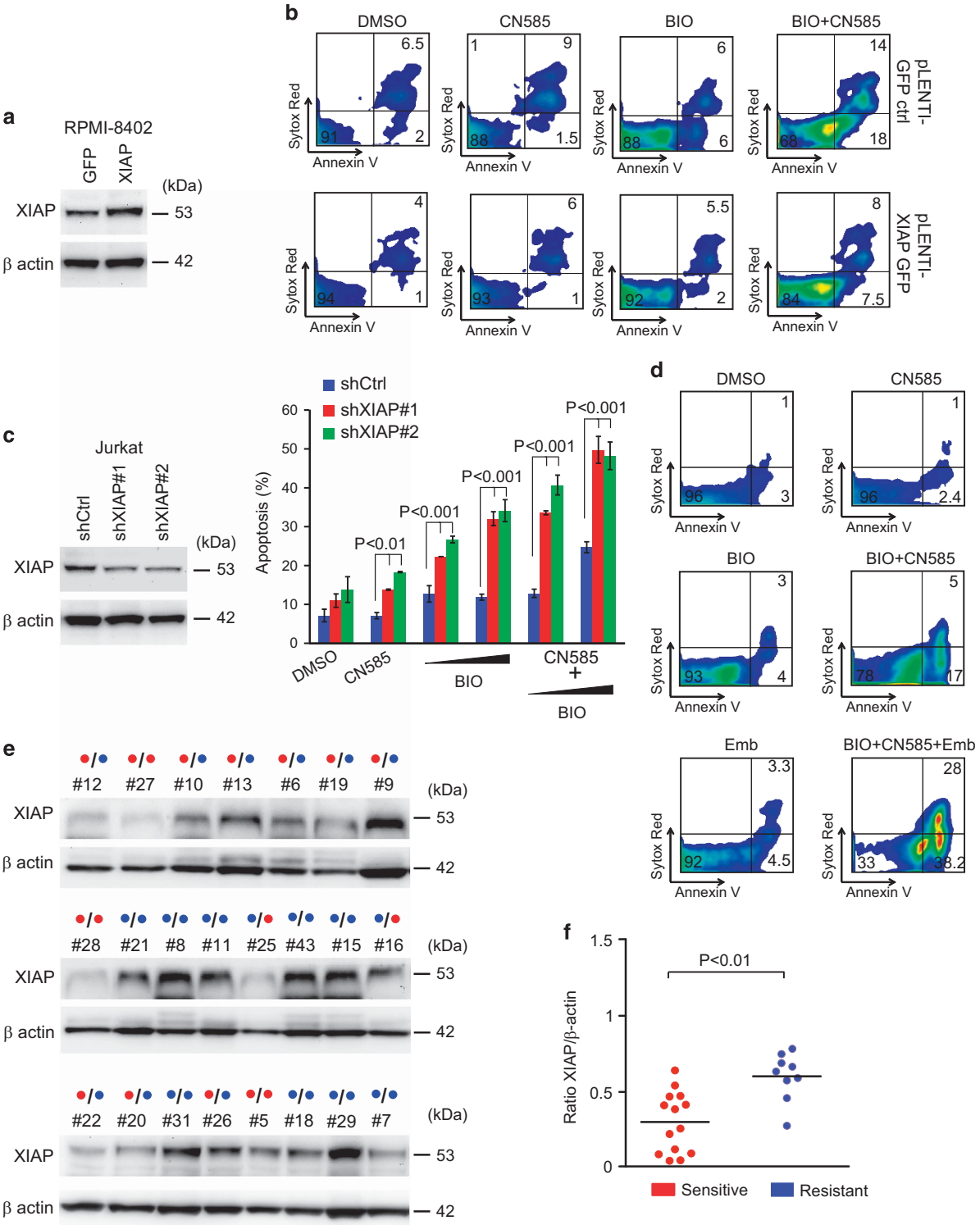

Figure 5. Modulation of XIAP expression by lentiviral vector-mediated overexpression or knockdown alters the apoptotic response to pharmacologic inhibition of Cn and GSK-3. XIAP expression levels (**a**) and representative plots of apoptosis (**b**) in RPMI 8402 cells stably expressing GFP or XIAP treated for 48 h with vehicle only, BIO, CN585 or BIO plus CN585 (BIO+CN585). (**c**) Jurkat cells were transduced with control vector (shCtrl) or vectors containing shRNA sequences against XIAP (shXIAP#1 and shXIAP#2). XIAP expression levels (left panel) and apoptotic quantification (right panel) in Jurkat cells transduced with shCtrl, shXIAP#1 and shXIAP#2 treated for 48 h with vehicle only, BIO (2–3 μM), CN585 (10 μM) or BIO plus CN585 (BIO+CN585; 2–3 and 10 μM, respectively). Error bars represent ± s.d. for triplicate experiments. (**d**) Representative plots of apoptosis in Jurkat cells treated with vehicle only, BIO, CN585, Embelin (Emb), BIO plus CN585 or BIO plus CN585 plus Emb. (**e**) Immunoblot analysis of XIAP expression in T-ALL xenografts. β-Actin is shown as loading control. Blue dots indicate resistance to treatment, while red dots indicate sensitivity to drug treatment. Left-most dot shows response to BIO treatment, while right-most dot shows response to CN585 treatment. (**f**) Graphical representation of XIAP/β-actin ratios in BIO- or CN585-sensitive (IC_{50} < 5 μM and IC_{50} < 20 μM, respectively) compared with BIO- and/or CN585-resistant (IC_{50} > 5 μM and IC_{50} ⩾ 20 μM, respectively) xenografts. Bars represent mean values. Expression of XIAP and β-actin was analyzed by immunoblotting (**a** and **c**).

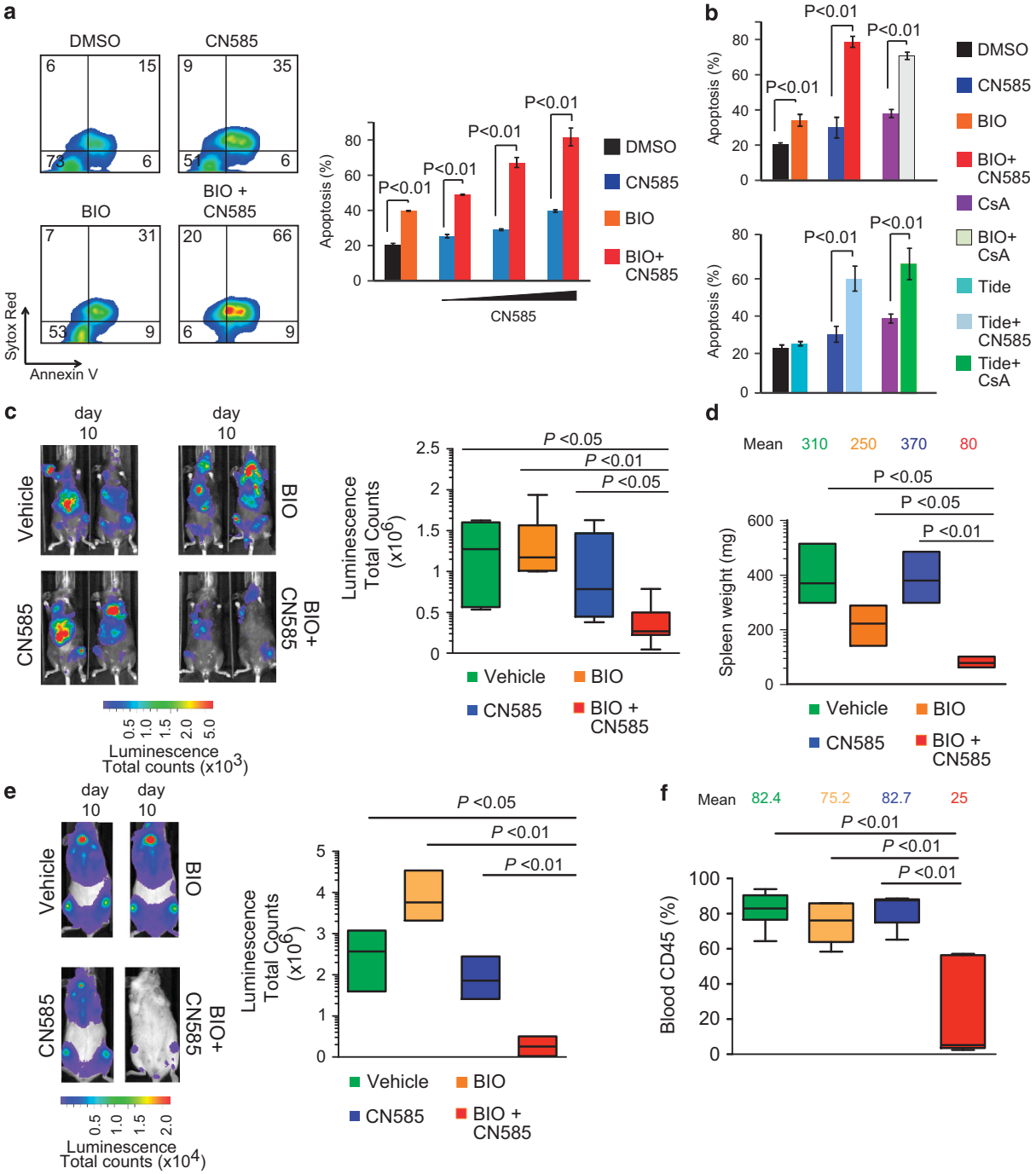

Figure 6. Pharmacologic inhibition of Cn and GSK-3 has potent anti-leukemic effects in models of T-ALL. (**a**) Left panels: representative plots of apoptosis in *NOTCH1*-induced mouse leukemia cells treated *in vitro* with vehicle only, BIO (1.5 μM), CN585 (10 μM) or BIO plus CN585 (BIO +CN585; 1.5 and 10 μM, respectively). Right panels: apoptotic quantification in *NOTCH1*-induced mouse leukemia cells treated with vehicle only, BIO (1.5 μM), CN585 (5–10 μM) alone or CN585 (5–10 μM) plus BIO (1.5 μM) in combination. Error bars represent ± s.d. for triplicate experiments. (**b**) Quantification of apoptosis in *NOTCH1*-induced mouse leukemia cells treated *in vitro* with vehicle only, BIO (1.5 μM), CN585 (10 μM), CsA (2 μg/ml) and Tideglusib (15 μM) in various combinations. Error bars represent ± s.d. of triplicate experiments. (**c**) Representative images (left panels) and quantitative analysis of treatment response by *in vivo* imaging (right panel) in mice allografted with *NOTCH1*-induced mouse leukemia cells treated with vehicle only, BIO (30 mg/kg), CN585 (30 mg/kg) or BIO (30 mg/kg) plus CN585 (30 mg/kg) on alternate days for 10 days. Each experimental group comprised of five to nine mice. The box plot whiskers extend from the lowest to the highest values. (**d**) Quantitative analysis by floating bars of tumor burden in each experimental group ($n = 3$) estimated by spleen weight in *NOTCH1*-induced mouse leukemic mice at the end of the 10-day treatment. (**e**) Representative images and analysis of treatment response by *in vivo* imaging (represented as floating bars) in nonobese diabetic/severe combined immunodeficiency IL2Rγ^{null} (NSG) mice xenografted with human T-ALL#28 expressing luciferase treated with vehicle only, BIO (30 mg/kg), CN585 (30 mg/kg) or BIO (30 mg/kg) plus CN585 (30 mg/kg) three times a week for 3 weeks starting from day 3 post-injection. Analysis after 10 days of treatment is shown. (**f**) Analysis of tumor burden in NSG mice xenografted with human T-ALL#28 expressing luciferase treated with vehicle only, BIO (30 mg/kg), CN585 (30 mg/kg) or BIO (30 mg/kg) plus CN585 (30 mg/kg) three times a week for 3 weeks, estimated by analyzing human CD45 (CD45) expression in peripheral blood lymphocytes after 21 days of engraftment. Box plot whiskers extend from the lowest to highest values.

inhibitory GSK-3β/α S9/21 phosphorylation is facilitated when T43 and S389/390 are phosphorylated. Conversely, GSK-3 enzymatic activity is maximal following phosphorylation on GSK-3β/α Y216/Y279, possibly through autophosphorylation.[11] The present study found PPP3CA to directly interact with GSK-3β and to increase its kinase activity, possibly through an activating interaction, which increases its autophosphorylation (pY216) and decreases pT43. Interestingly, a direct activating interaction between GSK-3β and p53 after DNA damage has been reported[23] and Cn has been shown to be able to dephosphorylate pS9 in neuroblast-derived cells but not in glioblast-derived cells.[8]

In certain cancers (skin cancer, oral cancer, esophageal cancer, breast cancer and lung cancer) GSK-3β has been reported to work as a tumor suppressor, whereas in others (pancreatic cancer, multiple myeloma, prostate cancer and *MLL* leukemia) it acts as a tumor promoter.[9,24] We found that ~40% (12/27) of primary T-ALL xenografts and >75% of T-ALL cell lines undergo loss of viability following GSK-3 inhibition with BIO (IC_{50} ⩽5 μM). Strikingly, sensitivity correlated with a low pS9/pY216 GSK-3β ratio and was more frequent in the immature pre/pro-T ALL subgroup. Persistent Cn/NFAT signaling has been shown to be pro-oncogenic *in vivo* in mouse models of human T-ALL/lymphoma[25] and CsA treatment *in vitro* has been demonstrated to be effective against ALL cells.[26] In addition, Cn has been shown to be essential for the ability of T-ALL leukemic cells to long-term propagate the disease in serial transplantation assays.[27] Interestingly, reports of tumor regression following CsA treatment in T-cell malignancies have been reported, further emphasizing the importance of the Cn-NFAT signaling axis in this disease.[28] Accordingly, we find that ~1/4 of primary (7/27) T-ALL xenografts (IC_{50} <20 μM) and ~60% of T-ALL cell lines (8/13) undergo loss of viability following Cn inhibition with CN585 (IC_{50} ⩽10 μM).

To our knowledge, the specific role of GSK-3 in normal T cells or in T-ALL cells has not been specifically addressed. On the basis of our findings, we propose that GSK-3 acts principally as a tumor promoter in T-ALL by promoting the stabilization of proteins such as MCL1, c-MYB and possibly XIAP (Supplementary Figure S8). Several GSK-3 substrates could have a role in the anti-proliferative/pro-apoptotic effects of joint GSK-3 and Cn inhibition seen in T-ALL cells.[15,29] In fact, GSK-3-mediated phosphorylation of β-catenin leads to β-catenin degradation, phosphorylation of PTEN by GSK-3 leads to PTEN destabilization,[30] phosphorylation of c-Myb by GSK-3 possibly leads to c-Myb stabilization[31] and phosphorylation of MCL1 by GSK-3 promotes FBXW7-mediated degradation of MCL1.[32] We find that in T-ALL cell lines and primary T-ALL xenografts GSK-3 inhibition leads to β-catenin stabilization, c-Myb degradation, does not significantly influence PTEN expression and promotes MCL1 degradation. Thus, in contrast to what has been described previously[32] we find that GSK-3 inhibition promotes MCL1 degradation in T-ALL cells. Possibly, different experimental conditions (type, dose and time of GSK-3 inhibition) and cell lines used in the two studies could have a role in explaining these differential findings. In addition, we found that the marked anti-leukemic effect of joint GSK-3 and Cn inhibition is mainly associated to the reduced expression of anti-apoptotic proteins such as XIAP and claspin, and to a lesser extent of survivin and clusterin. Association of XIAP overexpression with resistance to chemotherapy-induced apoptosis and poor outcome has been detected in several malignancies.[33] In addition, increased XIAP expression has been associated with poor prednisone response in T-ALL, with XIAP inhibition enhancing glucocorticoid-induced apoptosis.[34] We find that XIAP overexpression is associated with resistance to the apoptotic effects of GSK-3 and Cn inhibition, and that modulation of XIAP levels (pharmacological or genetic) is able to critically influence the capacity of T-ALL cells to undergo apoptosis following these drug treatments. Interestingly, the Smac mimetic BV6 has been reported to synergize with glucocorticoids in childhood ALL.[35] Thus, inhibition of apoptosis-suppressing molecules is emerging as an attractive therapeutic option in ALL and could exhibit a broad chemo-sensitization activity. Our preclinical studies using short-term treatment with BIO (to target GSK-3) and CN585 (to target Cn) in a murine model of NOTCH1-dependent leukemia provide promising evidence of efficacy. Similar results were obtained in a human T-ALL xenograft model using the same inhibitors and clinically relevant inhibitors such as Tideglusib and CsA. It is possible that therapy with GSK-3 inhibitor alone could deplete normal hematopoietic stem cells in addition to leukemic (stem?) cells dependent on GSK-3 activity, as GSK-3 seems necessary for self-renewal of normal hematopoietic stem cells.[36] Thus, combination therapy with an mammalian target of rapamycin inhibitor such as rapamycin may maintain the hematopoietic stem cell pool, while allowing the GSK-3 inhibitor and Cn inhibitor combination to deplete the leukemia cells for an effective therapy.

One note of caution is that prolonged combination therapy determined signs of toxicity; thus, the development of more specific inhibitors with suitable pharmacodynamic properties will be critical for future clinical trials.

CONFLICT OF INTEREST

The authors declare no conflict of interest.

ACKNOWLEDGEMENTS

This work was supported by the Italian Association for Cancer Research (AIRC) grants to AA (IG#14032) and VT (MFGA#13053); Ministero dell'Istruzione, dell'Università e della Ricerca (MIUR) Ex 60% to AA and EP; and Istituto Oncologico Veneto 5×1000 fund to AA. We are grateful to Adolfo A Ferrando for sharing cells and reagents, Jon Aster for the MigR1-*NOTCH1* L1601PΔP vector, Sonia Minuzzo and Marica Pinazza for providing T-ALL xenografts and Giorgia Pilotto for cell sorting.

AUTHOR CONTRIBUTIONS

VT performed and analyzed experiments. FB performed experiments. VA and SI provided primary T-ALL xenografts. JY performed bioinformatical analysis. GB provided primary T-ALL samples and clinical-immunophenotypical data. AA shared reagents and analyzed data. EP designed and performed experiments, directed research, analyzed data and wrote the paper. All the authors read and edited the manuscript.

REFERENCES

1 Bassan R, Hoelzer D. Modern therapy of acute lymphoblastic leukemia. *J Clin Oncol* 2011; **29**: 532–543.
2 Pui CH. Recent advances in acute lymphoblastic leukemia. *Oncology (Williston Park)* 2011; **25**: 341 346–347.
3 Buchholz M, Ellenrieder V. An emerging role for Ca2+/calcineurin/NFAT signaling in cancerogenesis. *Cell Cycle* 2007; **6**: 16–19.
4 Medyouf H, Ghysdael J. The calcineurin/NFAT signaling pathway: a novel therapeutic target in leukemia and solid tumors. *Cell Cycle* 2008; **7**: 297–303.
5 Buchholz M, Schatz A, Wagner M, Michl P, Linhart T, Adler G *et al.* Overexpression of c-myc in pancreatic cancer caused by ectopic activation of NFATc1 and the Ca2+/calcineurin signaling pathway. *EMBO J* 2006; **25**: 3714–3724.
6 Jauliac S, Lopez-Rodriguez C, Shaw LM, Brown LF, Rao A, Toker A. The role of NFAT transcription factors in integrin-mediated carcinoma invasion. *Nat Cell Biol* 2002; **4**: 540–544.
7 Pham LV, Tamayo AT, Yoshimura LC, Lin-Lee YC, Ford RJ. Constitutive NF-kappaB and NFAT activation in aggressive B-cell lymphomas synergistically activates the CD154 gene and maintains lymphoma cell survival. *Blood* 2005; **106**: 3940–3947.
8 Kim Y, Lee YI, Seo M, Kim SY, Lee JE, Youn HD *et al.* Calcineurin dephosphorylates glycogen synthase kinase-3 beta at serine-9 in neuroblast-derived cells. *J Neurochem* 2009; **111**: 344–354.
9 Wang Z, Smith KS, Murphy M, Piloto O, Somervaille TC, Cleary ML. Glycogen synthase kinase 3 in MLL leukaemia maintenance and targeted therapy. *Nature* 2008; **455**: 1205–1209.
10 Cross DA, Alessi DR, Cohen P, Andjelkovich M, Hemmings BA. Inhibition of glycogen synthase kinase-3 by insulin mediated by protein kinase B. *Nature* 1995; **378**: 785–789.

11 Wang X, Paulin FE, Campbell LE, Gomez E, O'Brien K, Morrice N *et al.* Eukaryotic initiation factor 2B: identification of multiple phosphorylation sites in the epsilon-subunit and their functions in vivo. *EMBO J* 2001; **20**: 4349–4359.
12 Sato N, Meijer L, Skaltsounis L, Greengard P, Brivanlou AH. Maintenance of pluripotency in human and mouse embryonic stem cells through activation of Wnt signaling by a pharmacological GSK-3-specific inhibitor. *Nat Med* 2004; **10**: 55–63.
13 Bene MC, Castoldi G, Knapp W, Ludwig WD, Matutes E, Orfao A *et al.* Proposals for the immunological classification of acute leukemias. European Group for the Immunological Characterization of Leukemias (EGIL). *Leukemia* 1995; **9**: 1783–1786.
14 Chou TC, Talalay P. Quantitative analysis of dose-effect relationships: the combined effects of multiple drugs or enzyme inhibitors. *Adv Enzyme Regul* 1984; **22**: 27–55.
15 Sutherland C. What are the bona fide GSK-3 substrates? *Int J Alzheimer Dis* 2011; **2011**: 505607.
16 Schimmer AD, Dalili S, Batey RA, Riedl SJ. Targeting XIAP for the treatment of malignancy. *Cell Death Differ* 2006; **13**: 179–188.
17 Yang Y, Fang S, Jensen JP, Weissman AM, Ashwell JD. Ubiquitin protein ligase activity of IAPs and their degradation in proteasomes in response to apoptotic stimuli. *Science* 2000; **288**: 874–877.
18 Erdmann F, Weiwad M, Kilka S, Karanik M, Patzel M, Baumgrass R *et al.* The novel calcineurin inhibitor CN585 has potent immunosuppressive properties in stimulated human T cells. *J Biol Chem* 2010; **285**: 1888–1898.
19 Chiang MY, Xu L, Shestova O, Histen G, L'Heureux S, Romany C *et al.* Leukemia-associated NOTCH1 alleles are weak tumor initiators but accelerate K-ras-initiated leukemia. *J Clin Invest* 2008; **118**: 3181–3194.
20 Shibasaki F, Price ER, Milan D, McKeon F. Role of kinases and the phosphatase calcineurin in the nuclear shuttling of transcription factor NF-AT4. *Nature* 1996; **382**: 370–373.
21 Graef IA, Mermelstein PG, Stankunas K, Neilson JR, Deisseroth K, Tsien RW *et al.* L-type calcium channels and GSK-3 regulate the activity of NF-ATc4 in hippocampal neurons. *Nature* 1999; **401**: 703–708.
22 Jope RS, Yuskaitis CJ, Beurel E. Glycogen synthase kinase-3 (GSK-3): inflammation, diseases, and therapeutics. *Neurochem Res* 2007; **32**: 577–595.
23 Watcharasit P, Bijur GN, Zmijewski JW, Song L, Zmijewska A, Chen X *et al.* Direct, activating interaction between glycogen synthase kinase-3beta and p53 after DNA damage. *Proc Natl Acad Sci USA* 2002; **99**: 7951–7955.
24 Mishra R. Glycogen synthase kinase 3 beta: can it be a target for oral cancer. *Mol Cancer* 2010; **9**: 144.
25 Medyouf H, Alcalde H, Berthier C, Guillemin MC, dos Santos NR, Janin A *et al.* Targeting calcineurin activation as a therapeutic strategy for T-cell acute lymphoblastic leukemia. *Nat Med* 2007; **13**: 736–741.
26 Ito C, Ribeiro RC, Behm FG, Raimondi SC, Pui CH, Campana D. Cyclosporin A induces apoptosis in childhood acute lymphoblastic leukemia cells. *Blood* 1998; **91**: 1001–1007.
27 Gachet S, Genesca E, Passaro D, Irigoyen M, Alcalde H, Clemenson C *et al.* Leukemia-initiating cell activity requires calcineurin in T-cell acute lymphoblastic leukemia. *Leukemia* 2013; **27**: 2289–2300.
28 Takemori N, Kodaira J, Toyoshima N, Sato T, Sakurai H, Akakura N *et al.* Successful treatment of immunoblastic lymphadenopathy-like T-cell lymphoma with cyclosporin A. *Leuk Lymph* 1999; **35**: 389–395.
29 Medina M, Wandosell F. Deconstructing GSK-3: the fine regulation of its activity. *Int J Alzheimer Dis* 2011; **2011**: 479249.
30 Maccario H, Perera NM, Davidson L, Downes CP, Leslie NR. PTEN is destabilized by phosphorylation on Thr366. *Biochem J* 2007; **405**: 439–444.
31 Kitagawa K, Hiramatsu Y, Uchida C, Isobe T, Hattori T, Oda T *et al.* Fbw7 promotes ubiquitin-dependent degradation of c-Myb: involvement of GSK-3-mediated phosphorylation of Thr-572 in mouse c-Myb. *Oncogene* 2009; **28**: 2393–2405.
32 Inuzuka H, Shaik S, Onoyama I, Gao D, Tseng A, Maser RS *et al.* SCF(FBW7) regulates cellular apoptosis by targeting MCL1 for ubiquitylation and destruction. *Nature* 2011; **471**: 104–109.
33 Tamm I, Richter S, Oltersdorf D, Creutzig U, Harbott J, Scholz F *et al.* High expression levels of x-linked inhibitor of apoptosis protein and survivin correlate with poor overall survival in childhood de novo acute myeloid leukemia. *Clin Cancer Res* 2004; **10**: 3737–3744.
34 Hundsdoerfer P, Dietrich I, Schmelz K, Eckert C, Henze G. XIAP expression is post-transcriptionally upregulated in childhood ALL and is associated with glucocorticoid response in T-cell ALL. *Pediatr Blood Cancer* 2010; **55**: 260–266.
35 Belz K, Schoeneberger H, Wehner S, Weigert A, Bonig H, Klingebiel T *et al.* Smac mimetic and glucocorticoids synergize to induce apoptosis in childhood ALL by promoting ripoptosome assembly. *Blood* 2014; **124**: 240–250.
36 Huang J, Zhang Y, Bersenev A, O'Brien WT, Tong W, Emerson SG *et al.* Pivotal role for glycogen synthase kinase-3 in hematopoietic stem cell homeostasis in mice. *J Clin Invest* 2009; **119**: 3519–3529.

Supplementary Information accompanies this paper on the Leukemia website (http://www.nature.com/leu)